Observation of a new high-pressure semimetal phase of GaAs from pressure dependence of the thermopower

2006 J. Phys.: Condens. Matter 18 L551

(http://iopscience.iop.org/0953-8984/18/42/L03)

INSTITUTE OF PHYSICS PUBLISHING JOURNAL OF PHYSICS: CONDENSED MATTER

J. Phys.: Condens. Matter **18** (2006) L551–L557 doi:10.1088/0953-8984/18/42/L03

LETTER TO THE EDITOR

Observation of a new high-pressure semimetal phase of GaAs from pressure dependence of the thermopower

Sergey V Ovsyannikov[1,2] **and Vladimir V Shchennikov**[1]

[1] High Pressure Group, Institute of Metal Physics of Russian Academy of Sciences, Urals Division, GSP-170, 18 S Kovalevskaya Street, Yekaterinburg 620041, Russia
[2] The Institute for Solid State Physics, The University of Tokyo, 5-1-5 Kashiwanoha, Kashiwa 277-8581, Chiba, Japan

E-mail: sergey@issp.u-tokyo.ac.jp

Received 9 August 2006, in final form 9 September 2006
Published 6 October 2006
Online at stacks.iop.org/JPhysCM/18/L551

Abstract

We report the use of the thermopower technique (Seebeck effect) as an effective tool for discovery of 'hidden' (for standard techniques, like x-ray, synchrotron, Raman, etc) phases of substances. Applying the thermopower technique to a set of GaAs single crystals pressurized in a sintered diamond anvil cell, we found an unknown high-pressure semimetal phase with the electron type of conductivity, similar to that recently discovered in ZnTe. A possible crystal structure of this phase is discussed. The pressure–temperature (P–T) phase diagrams of GaAs and ZnTe are compared.

(Some figures in this article are in colour only in the electronic version)

1. Introduction

Gallium arsenide, like silicon, is one of the most important semiconductors. The pressure-induced structural transformations in GaAs have already been studied by diffraction of x-ray and synchrotron radiation [1–6], Raman scattering [7], electrical resistance measurements [8, 9], optical transmittance [2], x-ray absorption [2], and electron microscopy [2]. At present, the sequence of the pressure-induced transitions in GaAs at room temperature in the pressure (P) range 0–20 GPa is supposed to be as follows: zinc blende (ZB) $\rightarrow$ orthorhombic *Cmcm* at $P \sim 11.2$–17.3 GPa under pressurization [10], and *Cmcm* $\rightarrow$ cinnabar $\rightarrow$ ZB at 11.9–15.1 and 8.1 GPa, respectively, under decompression [10]. Under P increase the cinnabar lattice transformed back to *Cmcm* [4], suggesting the possible stability of cinnabar on compression also [4, 11]. The simple-cubic phase with a 16-atom basis (SC16), predicted to be thermodynamically stable between the ZB and *Cmcm* phases, within 10.5–14.5 GPa [12–15], was found to appear only after heating of the *Cmcm* phase above 400 K at $P \sim 14$ GPa [5, 6]. Other predicted intermediate lattices, for example, NaCl near 16 GPa [16, 17], have not yet been observed.

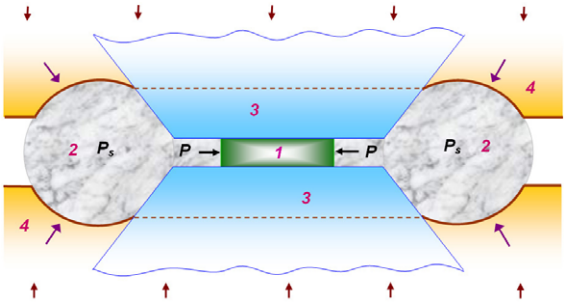

Figure 1. A sample in the high-pressure anvil cell. ***1***—sample, ***2***—gasket made of lithographic stone (soft $CaCo_3$-based material), ***3***—anvil insets (made of synthetic diamonds) in high-pressure plungers, ***4***—supporting hard-alloy matrixes (plungers). A ring-like bulge of the gasket ***2*** provides a supporting pressure P_s (up to 10 GPa) around the tips of anvils; high quasi-hydrostatic pressure P (from 0 up to 30 GPa) is created in a central part of the gasket around a sample [25]. The arrows show acting forces.

In A_NB_{8-N} compounds, the ZB, wurtzite and cinnabar lattices are semiconductors, the *Cmcm* and β-Sn ones are metals, while SC16 is a semimetal [12]. NaCl lattices were predicted to possess metallic properties [12]; however, this contradicted both with the significant optical energy gaps $E_g > 1$ eV [18] and with too high values of the thermopower S [19] found for ZnS, ZnSe, CdSe, etc. Calculations on the high-pressure phases of GaAs [11, 15] established that the cinnabar and the NaCl structures are a semiconductor with indirect gap $E_g = 0.26$ eV at $P \sim 16$ GPa, and a semimetal with the indirect overlapping of bands, respectively, while the SC16 lattice phase is a semiconductor with a direct zero gap. Therefore, techniques permitting the registration of pressure-driven peculiarities of electron structure may be helpful in the investigation of the phase transitions in GaAs. So, in the present work we applied the technique of high-pressure thermopower S (Seebeck effect) [20] for investigation of the semiconductor–metal (S–M) transition in GaAs at room temperature in a pressure range 0–20 GPa. S strongly depends on changes of both type and concentration of charge carriers [21–24], which makes it a powerful tool for the discovery of phases that are 'invisible' by standard techniques [23], such as x-ray diffraction and synchrotron diffraction, electrical resistance R and Raman scattering.

2. Experiment

The measurements of S and R under high quasi-hydrostatic pressure P were performed in synthetic diamond anvils of Bridgman type possessing a high electrical conductivity [25]. A gasket made of lithographic stone (soft $CaCO_3$-based material) served as a pressure-transmitting medium (figure 1). A sample of size $\sim 0.2 \times 0.2 \times 0.05$ mm^3 was put into a hole ~ 0.2 mm in diameter drilled in the gasket [20–24]. Synthetic diamond anvils were used both as electrical outputs to a sample and a heater–cooler pair (upper anvil was heated) [20–24]. To account for a possible contribution to S from the anvils themselves, we measured Pb samples ($S \approx -1.27$ μV K^{-1}) in the same conditions. The S values were measured in two regimes: at fixed P, from the linear dependence of thermoelectric voltage on the thermal difference ΔT along a sample, and at fixed ΔT (or density of thermal flux) under gradual variation of P. Values of P were estimated with an uncertainty less than 10% from a calibration curve based on the known pressure-induced phase transitions in Bi, GaP, ZnS, etc [20–24]. Decompression cycles were performed both to examine the reversibility of the phase transitions happening on pressurization, and to search for the traces of new phases, poorly visible (or invisible) under

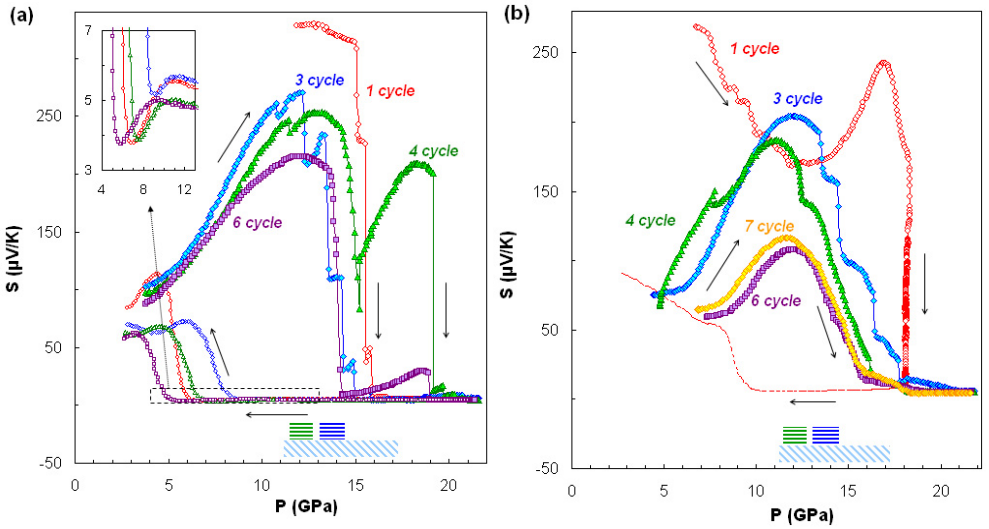

Figure 2. The pressure P dependences of the thermoelectric power S of n-GaAs (*No. 2*) (a) and p-GaAs (b) single crystals at $T = 295$ K. The upper dashed rectangles are the predicted regions of stability of the SC16 lattice ∼11.5–12.7 [14] and 13–14.5 GPa [11]; similar ranges were reported in [15]; the stability of the NaCl lattice was predicted near 16 GPa [16, 17]. The lower one is the beginning of the S–M transition near $P \sim 11.3$–17.2 GPa established by different techniques [10]. (a) The inset shows a large-scale part of the $S(P)$ curve at decompression, where a new phase (the 'dip' of thermopower) was seen for all cycles. (b) For *cycle 1* the S–M transition happened during ∼20 min exposure at fixed $P \sim 18$ GPa.

P increase. The phase transition pressures extracted from the decompression cycles were not used in the analysis. The relative errors in R and S determination did not exceed 5 and 20%, respectively. We investigated three single crystals, n-GaAs (no. 1 and no. 2 cut from the same ingot) with $n = 1 \times 10^{16}$ cm^{-3}, and p-GaAs doped with Zn with $p = 2.55 \times 10^{18}$ cm^{-3}.

3. Results and discussion

S was measured above $P \sim 4$–5 GPa, when R of a sample dropped to ∼200–300 kΩ; the sign of S corresponded to the hole type of conductivity (figures 2 and 3). A positive sign of S for all samples agreed with a direct/indirect band crossover happening in GaAs above ∼3 GPa, when the mobility of electrons as well as the electron contribution to conductivity decreased [26]. The behaviour of the $S(P)$ and $R(P)$ dependences attested to the S–M phase transition near ∼11–18 GPa (figures 2–4). The S–M transition pressure determined from the $S(P)$ and $R(P)$ curves seemed to be less in the n-type crystals than in p-type one. According to the x-ray diffraction data, the phase transition into the *Cmcm* phase was completed at $P \sim 20$–24 GPa [2, 4]. The small positive values of $S \sim +(7 \pm 3)$ μV K^{-1} at $P \sim 20$ GPa evidencing metal conductivity [9, 12] were close to those established previously for *Cmcm* high-pressure lattices of other $A_N B_{8-N}$ compounds [19].

Figures 2–4 demonstrate the large hysteresis of the forwards and backwards S–M transitions, consistent with the structural data [2, 4–6, 10, 12]. Such behaviour in semiconductors, including GaAs, is typically related to kinetic barriers that prevent or delay transformation into the equilibrium structure [12]. Because of the above kinetic barriers, substances may transform by an easier transition path via some stable (or metastable) structures

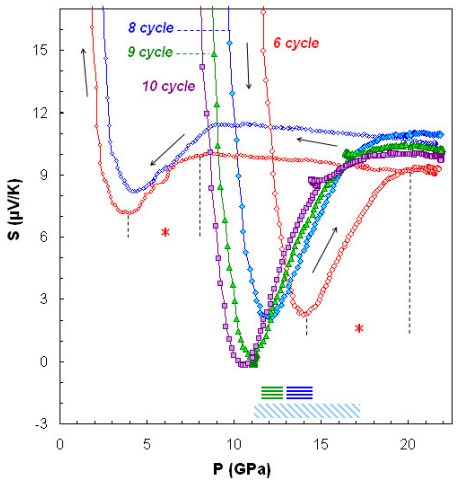

Figure 3. The large-scale parts of the pressure P dependences of the thermoelectric power S of n-GaAs (*No. 1*) at $T = 295$ K. The rectangles are the same as in figure 2. The dashed lines with an asterisk mark out the parts of $S(P)$, on the example of pressurization and decompression of *cycle 6*, where an unknown semimetal phase with the electron type of conductivity contributed to the total conductivity of heterophase mixture, consisting also of holes, ZB, *Cmcm*, and probably, cinnabar phases.

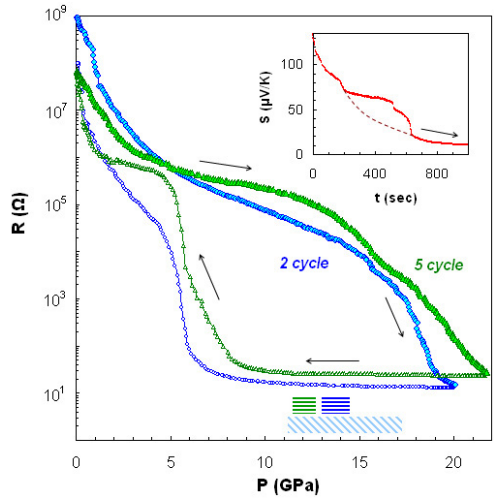

Figure 4. The pressure P dependences of electrical resistance R of p-GaAs at $T = 295$ K. The rectangles are the same as in figure 2. The 'stair' in $R(P)$ at decompression may be related to transient cinnabar phase. In the inset the time t dependence of the thermopower S at $P \sim 18$ GPa (figure 2(b), *cycle 1*) is given, attesting to the transition to a metastable semiconductor phase (probably, cinnabar); the dashed line shows the expected monotonic $S(t)$ dependence during the S–M transition in the absence of intermediate semiconductor phases.

(if any) [12]: tetrahedrally coordinated cinnabar in GaAs on decompression [1, 4]. Pressure-transmitting media also may be responsible for narrowing or extending of a hysteresis loop [2].

In a vicinity of the direct S–M transition, anomalies were noticed at $S(P)$ and $R(P)$ curves (figures 2 and 3). Earlier, a 'stair'-like peculiarity was already registered at $R(P)$ at the onset of the direct S–M transition [8, 9]. Such abrupt changes of $S(P)$ (as well as the wide range

of transition pressures found) might attest to competition between the phases with marginal stabilities.

From the close structural analogy established for the high-pressure lattices of ZnTe and GaAs [4, 12], we assumed that the abrupt increase of S (figure 2) at the onset of S–M transition might be due to the appearance of an intermediate semiconductor phase, supposedly with a cinnabar lattice [4], whose 'close to stability' region was predicted near $P \sim 16$ GPa [11]. The passing of a metastable semiconductor lattice during the direct S–M transition was seen also by a 'stair' in the dependence of thermopower on time $S(t)$ (inset in figure 4) recorded at fixed $P \approx 18$ GPa (figure 2(b), *cycle 1*). On decompression, the cinnabar phase might be assigned to the 'stair' in $R(P)$ (*cycle 5*, figure 4) and $S(P)$ (figure 2), as in the case of ZnTe [27, 28, 23]. The sign of S in the cinnabar phase of ZnTe is also positive [23] corroborating the above supposition.

The lowering of S down to zero and its inversion (figure 3, *cycles 9 and 10*) after the onset of the S–M transition pointed out the passing of one more intermediate phase with the electron type of conductivity. One might conclude that the electronic state found by the S 'dip' should be related to a new intermediate structural modification of GaAs; the time stability of this phase was examined by repeating the cycles and a long-term exposition at fixed P (figure 3, *cycle 9*, $P \sim 11$ GPa). This conclusion was supported by the recent discovery of the semimetal phase with the electron conductivity in ZnTe by the same 'dips' of $S(P)$ [23]; this phase of ZnTe was also established from the Raman spectra [29]. In case of GaAs no detectable Raman spectra were registered after the onset of the direct S–M transition, because the crystal turned out to be 'opaque to visible light' [2, 7].

By analogy with ZnTe, the semimetal conductivity of the new phase found was proposed [23]. This assumption was supported by the relatively high values of R and low values of S, that are typical neither for metals nor for semiconductors [19], while they may be characteristic for semimetals or semiconductors with a close to zero energy gap. According to the predictions this semimetal phase may have SC16 [12–15], NaCl [16, 17] or some other lattice structure [30]. As NaCl phases of other $A_N B_{8-N}$ compounds exhibit negative S (electron conductivity), such an attribution seemed reasonable. The structure of the similar intermediate n-type phase in ZnTe [23, 29, 31] has not been experimentally detected as yet, but it was predicted to be NaCl or SC16 also [23, 29, 31]. The calculated regions of stability of cinnabar, SC16, NaCl, and *Cmcm* lattices overlap each other [11–17, 32], and the difference between total energies of various possible lattices is comparable with the accuracy of calculations [11–17, 32, 33]. Usually there are kinetic barriers preventing transformation into an equilibrium structure, and the 'intermediary' phases (SC16, cinnabar, etc) with the easier transformation path may arise during the phase transitions from four-fold to six-fold coordination [12]; this explains the anomalous behaviour of electrical properties (R, S) during the S–M transition (figures 2–4). Also, elastic strains can significantly affect the boundaries of the phase stability and even change the type of structure of high-pressure phases [30].

Diffraction and Raman measurements at ultrahigh pressure are performed usually in a regime of discrete change of P, with a step ~0.5–1 GPa [1–7], so it seems hardly possible to detect phases with a narrow stability range. X-ray crystallographic techniques probe the long-range structural ordering of crystals, and usually register high-pressure phases already close to the completion of transformation [2, 10, 12]. The phase transition pressures estimated from x-ray data are indeed higher for the majority of compounds [2, 10, 12, 34], while R allows registering the beginning of transition [34, 35]. The $S(P)$ curve reflects S–M transition (under actions of P or T), ahead of R [34, 35] (at less pressures for P increase and at higher ones for P decrease), that explains advantages of $S(P)$ technique in registration of the phase transitions in case of GaAs.

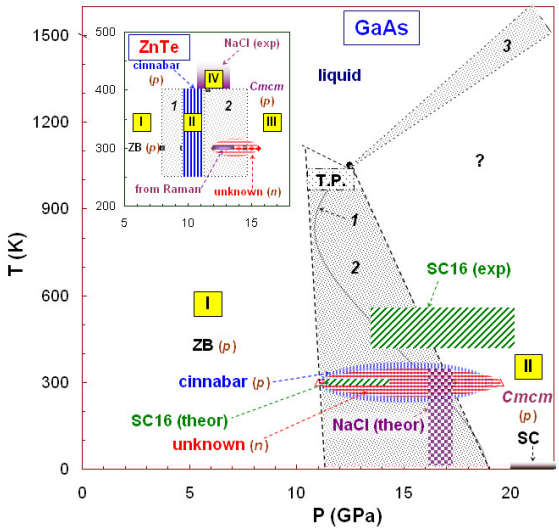

Figure 5. The schematic pressure–temperature (P–T) phase diagram of GaAs for the first cycle of pressurization. The diagram is based on the previous one from [2], where the phase boundaries of the liquid phase and the triple point (TP) were discussed. ***1*** marks the theoretical ZB–$Cmcm$ boundary taken from [36]; ***2*** the S–M transition region (from [2]) (at $T = 295$ K, $11.3 \leqslant P \leqslant 17.4$ GPa [10]); ***3*** the assumed melting curve of the high-pressure phase, from [2, 36]. **I** and **II** denote the regions of thermodynamic stability of GaAs-I (zinc blende) and GaAs-II (orthorhombic *Cmcm*); p and n labels near a phase notation mean the type of conductivity (holes or electrons, respectively). We marked the widest ranges, where the contributions of the new phases (SC16, cinnabar, semimetal) were noticed. Both in the theoretical and experimental studies, the influence of temperature on the transformation path was not investigated, though it seems significant as several possible phases have similar energies. Other remarks: (i) The ZB modification irrespectively of doping (p, n) is a hole semiconductor above $P \sim 3$–4 GPa. (ii) The cinnabar phase is a hole semiconductor. In the present study we proposed it to be metastable against the unknown semimetal phases with electron conductivity. A stable cinnabar phase was found to be present only on decompression [4]. (iii) The unknown semimetal phase probably crystallizes in NaCl or SC16 lattices. The predicted stability regions for SC16 ($P \sim 11$–14.5 GPa [12–15]) GPa and NaCl (near $P \sim 16$ GPa [16, 17]) are also shown. (iv) SC16 (exp) denotes an approximate region where SC16 lattice of GaAs was experimentally observed by heating of either ZB or *Cmcm* lattices [5, 6]. Its observation opened a question about the crystal structure above 500–600 K. (v) The transition into the orthorhombic *Cmcm* lattice is completed at $P \sim 20$–24 GPa [2, 4], so region **II** may contain small fractions of all the above-mentioned phases. (vi) SC is the superconducting phase with a critical temperature $T_c \sim 4.5$ K at $P \sim 20$ GPa; then T_c decreases with pressure to 3 K at $P \sim 48$ GPa [9]. (vii) Decompression from the SC16 lattice led to the wurtzite structure of GaAs, stable at ambient conditions [6], while cooling of the high-pressure *Cmcm* phase and sequential decompression resulted in amorphous and microcrystalline phases [37]. In the inset the central part of the P–T diagram of ZnTe is shown [38]; **I**, **II**, **III** and **IV** correspond to ZB, cinnabar and orthorhombic *Cmcm* and NaCl phases, respectively, and 1 and 2 to the transition regions from **I**–**II**, and **II**–**III** phases, respectively. An unknown semimetal phase was observed during the transition from cinnabar into the *Cmcm* phase [23]. One can see an analogy between the diagrams of ZnTe and GaAs, while the phases found under heating are different, NaCl in ZnTe [38], and SC16 in GaAs [5, 6].

4. Conclusion

The behaviour of S reflects real pressure-driven changes in the electron structure which are 'hidden' for other techniques. The new phase found pointed at a close similarity of GaAs with other $A_N B_{8-N}$ semiconductors, where the NaCl phase exists between cinnabar and

orthorhombic *Cmcm* ones. On decompression, the transition sequence in GaAs may look similar to that in ZnTe [23, 29, 31]:, orthorhombic *Cmcm* → unknown semimetal phase → cinnabar → ZB. Meanwhile, according to the anomalies in $S(P)$ (see figures 2 and 3), for pressurization one can expect also (co-) existence of alternative paths, where only one intermediate phase forms, cinnabar (as proposed in [4, 11]) or the revealed semimetal (SC16 in [12–15], NaCl in [16, 17]) (figure 5).

We thank Drs G A Matveev, G M Minkov (IMP), and O Rut (Urals State University) for the samples kindly provided. The work was supported by the RFBR, Grant No. 04-02-16178.

References

[1] Weir S T, Vohra Y K, Vanderborgh C A and Ruoff A L 1989 *Phys. Rev.* B **39** 1280
[2] Besson J M, Itie J P, Polian A, Weill G, Mansot J L and Gonzalez J 1991 *Phys. Rev.* B **44** 4214
[3] Nelmes R J, McMahon M I, Wright N G, Allan D R, Liu H and Loveday J S 1995 *J. Phys. Chem. Solids* **56** 539
[4] McMahon M I and Nelmes R J 1997 *Phys. Rev. Lett.* **78** 3697
[5] McMahon M I, Nelmes R J, Allan D R, Belmonte S A and Bovornratanaraks T 1998 *Phys. Rev. Lett.* **80** 5564
[6] McMahon M I and Nelmes R J 2005 *Phys. Rev. Lett.* **95** 215505
[7] Venkateswaran U D, Cui L J, Weinstein B A and Chambers F A 1991 *Phys. Rev.* B **43** 1875
Venkateswaran U D, Cui L J, Weinstein B A and Chambers F A 1992 *Phys. Rev.* B **45** 9237
[8] Minomura S and Drickamer H G 1962 *J. Phys. Chem. Solids* **23** 451
[9] Zhang S B, Erskine D, Cohen M L and Yu P Y 1989 *Solid State Commun.* **71** 369
[10] Mujica A, Rubio A, Munoz A and Needs R J 2003 *Rev. Mod. Phys.* **75** 863
[11] Kelsey A A, Ackland G J and Clark S J 1998 *Phys. Rev.* B **57** R2029
[12] Ackland G J 2001 *Rep. Prog. Phys.* **64** 483
[13] Crain J, Piltz R O, Ackland G J, Payne M C, Milman V, Lin J S, Hatton P D, Nam Y H and Clark S J 1994 *Phys. Rev.* B **50** 8389
[14] Mujica A, Needs R J and Munoz A 1995 *Phys. Rev.* B **52** 8881
[15] Arabi H, Pourghazi A, Ahmadian F and Nourbakhsh Z 2006 *Physica* B **373** 16
[16] Froyen S and Cohen M L 1983 *Phys. Rev.* B **28** 3258
[17] Lu L Y, Chen X R, Yu B R and Gou Q Q 2006 *Chin. Phys.* **15** 802
[18] Goni A R and Syassen K 1998 *Semicond. Semimet.* **54** 247
[19] Ovsyannikov S V and Shchennikov V V 2004 *Physica* B **344** 190
[20] Tsidil'kovkii I M, Shchennikov V V and Gluzman N G 1983 *Sov. Phys.—Semicond.* **17** 604
[21] Ovsyannikov S V, Shchennikov V V, Ponosov Y S, Gudina S V, Guk V G, Skipetrov E P and Mogilenskikh V E 2004 *J. Phys. D: Appl. Phys.* **37** 1151
[22] Shchennikov V V, Ovsyannikov S V, Misiuk A and Shchennikov V V Jr 2004 *Phys. Status Solidi* b **241** 3242
[23] Ovsyannikov S V and Shchennikov V V 2004 *Solid State Commun.* **132** 333
[24] Ovsyannikov S V, Shchennikov V V, Kar'kin A E and Goshchitskii B N 2005 *J. Phys.: Condens. Matter* **17** S3179
[25] Shchennikov V V 1990 A device for producing of ultrahigh pressure *SU Patent Specification* 1762457
[26] Pitt G D 1977 *Contemp. Phys.* **18** 137
[27] Samara G A and Drickamer H G 1962 *J. Phys. Chem. Solids* **23** 457
[28] Ohtani A, Motobayashi M and Onodera A 1980 *Phys. Lett.* A **75** 435
[29] Camacho J, Loa I, Cantarero A and Syassen K 2002 *J. Phys.: Condens. Matter* **14** 739
[30] Durandurdu M 2006 *J. Phys.: Condens. Matter* **18** 4887
[31] Gangadharan R, Jayalakshmi V, Kalaiselvi J, Mohan S, Murugan R and Palanivel B 2003 *J. Alloys Compounds* **359** 22
[32] Rino J P, Chatterjee A, Ebbsjo I, Kalia R K, Nakano A, Shimojo F and Vashishta P 2002 *Phys. Rev.* B **65** 195206
[33] Durandurdu M and Drabold D A 2002 *Phys. Rev.* B **66** 045209
[34] Shchennikov V V, Ovsyannikov S V and Frolova N Y 2003 *J. Phys. D: Appl. Phys.* **36** 2021
[35] Shchennikov V V, Ovsyannikov S V, Vorontsov G V and Shchennikov V V Jr 2004 *Phys. Status Solidi* b **241** 3203
[36] Van Vechten J A 1973 *Phys. Rev.* B **7** 1479
[37] Tsuji K, Katayama Y, Yamamoto Y, Kanda H and Nosaka H 1995 *J. Phys. Chem. Solids* **56** 559
[38] San-Miguel A, Polian A, Gauthier M and Itié J P 1993 *Phys. Rev.* B **48** 8683